

1 **Chromosome size affects sequence divergence between species through the interplay of**
2 **recombination and selection**

3 Anna Tigano^{1,2*#}, Ruqayya Khan³, Arina D. Omer³, David Weisz³, Olga Dudchenko^{3,4}, Asha S. Multani⁵,
4 Sen Pathak⁵, Richard R. Behringer⁵, Erez L. Aiden^{3,4,6,7,8}, Heidi Fisher⁹, Matthew D. MacManes^{1,2}

5

6 ¹University of New Hampshire, Molecular, Cellular, and Biomedical Sciences Department,
7 Durham, NH 03824, USA

8 ²Hubbard Center for Genome Studies, University of New Hampshire, Durham, NH 03824, USA

9 ³The Center for Genome Architecture, Department of Molecular and Human Genetics,

10 Baylor College of Medicine, Houston, TX 77030, USA

11 ⁴Department of Computer Science, Department of Computational and Applied Mathematics,

12 Rice University, Houston, TX 77030, USA

13 ⁵Department of Genetics, University of Texas, M.D. Anderson Cancer Center, Houston, TX 77030, USA

14 ⁶Center for Theoretical and Biological Physics, Rice University, Houston, TX 77030, USA

15 ⁷Shanghai Institute for Advanced Immunochemical Studies, ShanghaiTech University, Shanghai

16 201210, China

17 ⁸School of Agriculture and Environment, University of Western Australia, Perth, WA 6009,

18 Australia

19 ⁹Department of Biology, University of Maryland, College Park, MD 20742, USA

20 *corresponding author: anna.tigano@unh.edu

21 #current affiliation: University of British Columbia Okanagan, Kelowna, BC V1V 1V7, Canada

22

23 Keywords: mammal, genome assembly, *Peromyscus*, *Mus*, great apes, genome evolution

24

25

26

27 **Abstract**

28 The structure of the genome shapes the distribution of genetic diversity and sequence divergence. To
29 investigate how the relationship between chromosome size and recombination rate affects sequence
30 divergence between species, we combined empirical analyses and evolutionary simulations. We estimated
31 pairwise sequence divergence among 15 species from three different Mammalian clades - *Peromyscus*
32 rodents, *Mus* mice, and great apes - from chromosome-level genome assemblies. We found a strong
33 significant negative correlation between chromosome size and sequence divergence in all species
34 comparisons within the *Peromyscus* and great apes clades, but not the *Mus* clade, suggesting that the
35 dramatic chromosomal rearrangements among *Mus* species may have masked the ancestral genomic
36 landscape of divergence in many comparisons. Our evolutionary simulations showed that the main factor
37 determining differences in divergence among chromosomes of different size is the interplay of
38 recombination rate and selection, with greater variation in larger populations than in smaller ones. In
39 ancestral populations, shorter chromosomes harbor greater nucleotide diversity. As ancestral populations
40 diverge, diversity present at the onset of the split contributes to greater sequence divergence in shorter
41 chromosomes among daughter species. The combination of empirical data and evolutionary simulations
42 revealed that chromosomal rearrangements, demography, and divergence times may also affect the
43 relationship between chromosome size and divergence, and deepen our understanding of the role of
44 genome structure on the evolution of species divergence.

45 **Introduction**

46 Chromosomes are the fundamental unit of inheritance of the nuclear DNA in all eukaryotic species and
47 their evolution goes arm in arm with organismal evolution. Not only the sequence, but also the size,
48 shape, structure, and number of chromosomes can vary between species, populations, and even
49 individuals within a population (Hauffe and Searle 1993; Graphodatsky et al. 2011; Dion-Côté et al.
50 2017; Moura et al. 2020). Chromosome evolution is therefore crucial to our understanding of the
51 evolution and maintenance of biodiversity. Despite this, our current understanding of these relationships
52 is limited. The rapidly increasing number of chromosome-level genome assemblies has started to shed
53 light on the role of chromosomes in the genomic distribution of genetic diversity within and between
54 species. For example, chromosome structure, including the location of telomeres or centromeres, can be a
55 strong predictor of the position of dips and peaks in nucleotide diversity (π) and sequence divergence (d)
56 within a chromosome (Butlin 2005; Smukowski and Noor 2011; Burri et al. 2015; Sardell et al. 2018;
57 Tigano et al. 2021; Robinson et al. 2021). The heterogeneous distribution of π and d in the genome is
58 apparent among chromosomes too (Dutoit et al. 2017; Murray et al. 2017; Henderson and Brelsford 2020;
59 Robinson et al. 2021), but the role of genome structure in generating this distribution, including the
60 number and size of chromosomes in a genome, is less clear.

61 To avoid the production of aberrant gametes, the correct segregation of chromosomes during
62 meiosis requires that chromosomes undergo at least one cross-over per event (Mather 1938; Hassold and
63 Hunt 2001), which results in shorter chromosomes experiencing overall proportionally higher
64 recombination rates. In fact, a significant relationship between chromosome size and recombination rate
65 has been reported in many species (but not all) from fungi to mammals (Kaback et al. 1992; Jensen-
66 Seaman et al. 2004; Pessia et al. 2012; Farré et al. 2013; Kawakami et al. 2014; Haenel et al. 2018).
67 Chromosome size is also inversely correlated with π in some species of birds and mammals (Dutoit et al.
68 2017; Murray et al. 2017; Tigano et al. 2020; Robinson et al. 2021), but not others (Pessia et al. 2012;
69 Dutoit et al. 2017). Further, higher d in microchromosomes (< 20 Mb) relative to macrochromosomes (>
70 40 Mb) has been observed in several bird species (Delmore et al. 2018). While these studies highlight the

71 intricate relationship between chromosome size, recombination rate, nucleotide diversity, and sequence
72 divergence, many other factors likely contribute to this relationship. Currently, our understanding of these
73 additional factors is limited by both theory and lack of empirical data.

74 Investigating the factors shaping the levels and patterns of sequence divergence between species
75 is fundamental to understand the molecular mechanisms underlying the process of adaptation and
76 speciation. Nonetheless, the relative contribution of recombination to divergence among species has
77 rarely been directly investigated, especially at the chromosome scale, in species other than humans and
78 their closest relatives, the great apes (Hellman et al. 2003; Phung et al. 2016). However, a recent study
79 used chromosome size as a proxy for recombination rate to test how genome structure affected divergence
80 among eight avian sister species pairs, and reported significantly higher divergence in microchromosomes
81 than in macrochromosomes (Delmore et al. 2018), but it did not address the mechanisms underpinning
82 this relationship.

83 Although the correlation between recombination rate and π has often been reported (Begun and
84 Aquadro 1992; Nachman 2001; Cutter and Choi 2010), the factors and their relative roles in determining
85 this relationship are less clear (Ellegren and Galtier 2016). Non-crossover gene conversion (gene
86 conversion hereafter) and selection, including linked selection, are among the factors most commonly
87 invoked to explain the correlation between recombination and π . Gene conversion is the process by which
88 double-strand DNA breaks during meiosis are repaired using homologous sequence as template without
89 crossing-over, and although it affects shorter sequences than other types of crossing-over events do, it can
90 increase diversity and affect divergence among populations and species (Korunes and Noor 2017). Under
91 a purely neutral model of evolution, π is determined by the effective population size (N_e) and the mutation
92 rate (μ), as expressed by the equation $\pi=4N_e\mu$ (Tajima 1983). In this model, higher recombination rate
93 may increase π in smaller chromosomes if recombination results in the introduction of mutations through
94 gene conversion (Coop and Przeworski 2007; Arbeithuber et al. 2015). For example, a study on humans
95 showed a correlation between recombination, diversity, and divergence to the chimpanzee and the
96 baboon, and explained these relationships with a pure neutral model entailing recombination-associated

97 variation in mutation rates (Hellmann et al. 2003). In contrast, under a non-neutral evolutionary model,
98 selection reduces diversity in the genomic regions surrounding beneficial or deleterious mutations via
99 selective sweeps and background selection, respectively, with a greater diversity-reducing effect in areas
100 of low recombination (Smith and Haigh 1974; Wiehe and Stephan 1993; Hudson and Kaplan 1995), even
101 though purifying selection can also counteract the loss of diversity due to background selection by
102 associative overdominance if the deleterious variant is recessive (Ohta 1971; Gilbert et al. 2020). Support
103 for the role of selection comes from another study on humans, showing how background selection in the
104 ancestral population affects neutral divergence by reducing diversity in the sites close to selected sites
105 (Phung et al. 2016). At the chromosome level, at least in humans, both gene conversion and linked
106 selection may therefore contribute to the higher diversity reported in smaller chromosomes, though the
107 generality of these findings is still limited to humans and few other species.

108 How can variation in mean recombination rate explain differences in divergence across
109 chromosomes of varying size? The relationship between recombination and divergence could be
110 explained by variation in ancestral polymorphism. Selection and/or mutagenic recombination in the
111 ancestral population may lead to variation in genetic diversity across the genome (see above), and when
112 this population splits into two populations, the initial differences between these daughter populations
113 simply reflect patterns of diversity present in the parent population. Heterogeneous levels of diversity
114 across the genome of ancestral populations hence may give rise to variation in divergence among
115 chromosomes of different sizes between daughter populations. Alternatively, higher recombination could
116 increase divergence by leading to the accumulation of more mutations between diverging populations,
117 and hence affect divergence directly. As mutagenic and selective forces before and after splitting are not
118 mutually exclusive and could both explain the effect of recombination on divergence (Kulathinal et al.
119 2008), it is crucial to understand the factors that shape the distribution of diversity across the genome.

120 The analysis of chromosome-level patterns of diversity and divergence are now possible thanks to
121 the increasing number of high-quality, chromosome-level assemblies available for several closely-related
122 species within a clade. Great apes and *Mus* mice were the first mammalian clades with sufficient genomic

123 resources to enable genome-scale comparative genomics analyses (Thybert et al. 2018). For example,
124 while within humans and among great apes, fine-scale diversity and divergence seem to be correlated
125 with recombination, and recombination with chromosome size (Hellmann et al. 2003; Jensen-Seaman et
126 al. 2004), these relationships are weaker or not present in the house mouse *Mus musculus* (Jensen-Seaman
127 et al. 2004; Kartje et al. 2020). Great apes and *Mus* mice are phylogenetically distant, with an estimated
128 last common ancestor ~90 million years ago (timetree.org), and differ in genome size, 3.1 Gb and 2.6 Gb
129 for the human and the *Mus musculus* genomes, respectively. Furthermore, they differ substantially in their
130 degree of genome structure conservation, with only one major chromosomal fusion in humans compared
131 to the other great apes (2n=46-48) and extreme variation in chromosome number in *Mus* mice (2n=22-48;
132 Hauffe and Searle 1993). Although rodents of the genus *Peromyscus* look similar to *Mus* mice in
133 appearance and have similar genome sizes, they last shared a common ancestor with *Mus* ~25 million
134 years ago (Steppan et al. 2004) and have very karyotypically stable genomes (2n=48; Smalec et al. 2019),
135 even more so than great apes. As a rodent lineage with increasing genomic resources (Colella et al. 2020;
136 Tigano et al. 2020; Colella et al. 2021) and conserved genome structure, *Peromyscus* offers similarities
137 and contrasts to both the *Mus* and the great apes lineages, thus representing an ideal third clade to
138 understanding the role of genome structure stability and the relationships between chromosome size,
139 recombination, diversity, and divergence in mammals. For example, similar to the great apes (Hellman et
140 al. 2003) but contrasting with *M. musculus*, the cactus mouse (*Peromyscus eremicus*) shows a strong
141 inverse correlation between chromosome size and π (Tigano et al. 2020); conserved synteny,
142 recombination rates, and crossover patterning among *Peromyscus* species (Peterson et al. 2019; Smalec et
143 al. 2019) together suggest that this relationship between chromosome size and π may be common among
144 species in this genus. In light of these observations on the correlation (or lack thereof) between π and
145 chromosome size, we hypothesize that also d will show a negative relationship with chromosome size in
146 great apes and *Peromyscus* but not in *Mus*.

147 By combining the analysis of chromosome-level genome assemblies from three different
148 mammalian clades - *Mus* spp., *Peromyscus* spp., and great apes - and individual-based evolutionary

149 simulations, we tested a) whether chromosomes of different sizes show different levels of sequence
150 divergence among species within a clade and b) the evolutionary, demographic, and molecular factors
151 linking recombination, diversity within species, and divergence among species. Through evolutionary
152 simulations, we tested the role of recombination, effective population size N_e , severity of bottleneck
153 associated with population splitting, gene conversion, selection, divergence time, and the interplay of
154 these factors in generating and maintaining genetic diversity and divergence. Our results show that
155 heterogeneous recombination rates across the genome and their interplay with selection and demographic
156 factors affect genetic diversity and divergence not only at a small scale within a chromosome, but also at
157 a broad scale among chromosomes of different lengths, thus providing new and important insights into
158 the role of genome structure, and potentially chromosomal rearrangements, in the heterogeneous
159 distribution of genetic diversity and divergence within and between species. These findings are
160 foundational to our understanding of the process of speciation and adaptation, and highlight the
161 importance of considering the structure and the heterogeneous distribution of recombination rates of the
162 genome for the inference of selective sweeps and demographic histories.

163

164 **Methods**

165 *Analyses of divergence*

166 We examined chromosome-level reference genomes for four *Mus* species (*M. musculus*, *M. spretus*, *M.*
167 *caroli*, and *M. pahari*), five great apes (*Homo sapiens*, *Pan troglodytes*, *Pan paniscus*, *Gorilla gorilla*,
168 and *Pongo abelii*), and six *Peromyscus* species (*P. maniculatus*, *P. polionotus*, *P. eremicus*, *P. crinitus*, *P.*
169 *nasutus*, and *P. californicus*; Accession numbers in Table S1). Reference genomes for all these species
170 were publicly available, except for *P. nasutus* and *P. californicus*, which we *de novo* assembled using a
171 combination of sequencing approaches and final chromosome-scaffolding with Hi-C data. For *P. nasutus*,
172 we obtained a tissue sample from a female individual collected at El Malpais National Conservation Area
173 (New Mexico, USA) and stored at the Museum of Southwestern Biology (MSB:Mamm:299083). We
174 extracted high molecular weight DNA with the MagAttract HMW DNA Kit (QIAGEN) and selected long

175 fragments (> 10 kb and progressively above 25 kb) using a Short Read Eliminator Kit (Circulomics Inc.).
176 A 10X Genomics linked-read library was generated using this high-quality DNA sample at Dartmouth
177 Hitchcock Medical Center (New Hampshire, USA) and sequenced at Novogene (California, USA) using
178 one lane of 150 bp paired-end reads on an Illumina HiSeq X sequencing platform. We produced a first
179 draft of the *P. nasutus* genome assembly using *Supernova 2.1.1* (Weisenfeld et al. 2017) with default
180 settings and these linked reads as input. To order and orient scaffolds in chromosomes we generated and
181 sequenced a proximity-ligation library (Hi-C) from the same sample used for the 10X library as part of
182 the DNA Zoo consortium effort (dnazoo.org). The Hi-C data were mapped to the 10X assembly with
183 Juicer (Durand et al. 2016) and scaffolds were ordered and oriented in chromosomes with the *3D-DNA*
184 pipeline (Dudchenko et al. 2017) and Juicebox Assembly Tools (Dudchenko et al.). The Hi-C data are
185 available on www.dnazoo.org/assemblies/Peromyscus_nasutus and can be visualized using Juicebox.js, a
186 cloud-based visualization system for Hi-C data (Robinson et al. 2018). For the *P. californicus* genome,
187 high molecular weight DNA was extracted from liver tissue from a captive female individual from a
188 colony maintained at the University of Maryland (USA) and sequenced using 10X Genomics technology
189 at the UC Davis Genome Center (California, USA). A first draft genome for *P. californicus* was based on
190 these 10X linked reads and assembled using *Supernova* as for *P. nasutus*. Then, Chicago and Dovetail Hi-
191 C libraries were created by Dovetail Genomics (California, USA) and used to scaffold the draft assembly
192 with the HiRise pipeline. The Chicago data were used first and the resulting improved assembly was used
193 as input for a second round of scaffolding with the Hi-C data only. The alignment of several *Peromyscus*
194 genomes revealed some assembly errors in the existing *P. eremicus* assembly (Tigano et al. 2020), so we
195 generated an additional Hi-C library from a primary fibroblast collection at the T.C. Hsu Cryo-Zoo at the
196 University of Texas MD Anderson Cancer Center. Using the new data, we performed misjoin correction
197 and re-scaffolding using *3D-DNA* (Dudchenko et al., 2017) and Juicebox Assembly Tools (Dudchenko et
198 al., 2018). The new Hi-C data for *P. eremicus* are available on
199 www.dnazoo.org/assemblies/Peromyscus_ereamicus and are visualized using Juicebox.js (Robinson et al.
200 2018). Although the misassemblies present in the previous *P. eremicus* genome assembly were

201 intrachromosomal and did not greatly affect estimates of sequence divergence at the chromosome-level,
202 here we report divergence estimates based on the more accurate assembly.

203 We generated pairwise alignments and estimated sequence divergence (d) with *Mummer4*
204 (Marçais et al. 2018) and custom scripts (https://github.com/atigano/mammal_chromosome_size). First,
205 we aligned pairs of genomes in each clade with *nucmer*, randomly choosing one as the reference and the
206 other as the query, and the settings `--maxgap 2000` and `--mincluster 1000`. We retained a global set of
207 alignments (`-g`) longer than 10 kb using *delta-filter* and converted the output into ‘btab’ format using
208 *show-coords*. To identify and exclude N-to-N matches from downstream analyses we based our analyses
209 on the estimated ‘percent similarity’ rather than ‘percent identity’. As percent similarities were calculated
210 for alignments of different lengths, we calculated weighted mean chromosome-level d ($= 1 - (\text{percent}$
211 $\text{similarities})$) for each chromosome correcting for alignment length. For the purpose of this study, we
212 focused on autosomes and excluded estimates for sex chromosomes, when present in the genome
213 assembly, because sex chromosomes experience a different combination of evolutionary forces than do
214 autosomes. We tested the ability of the \log_{10} -transformed chromosome size in bp (explanatory variable) to
215 predict mean chromosome-level divergence (response variable) separately for each species pairwise
216 alignment using linear models (simple linear regressions), and plotted these relationships in R version
217 3.6.2 (R core team).

218

219 *Evolutionary simulations*

220 To disentangle the factors contributing to the relationship between chromosome size, recombination,
221 diversity and divergence, we performed individual-based time-forward evolutionary simulations in
222 SLiM3 (Haller and Messer 2019). We simulated individuals using a Wright-Fisher model, where an
223 ancestral population (pop_A) splits into two populations (pop_1 and pop_2) after $20N_e$ generations (Fig. S1A),
224 and prevented gene flow between diverging populations pop_1 and pop_2 to control for this potential
225 confounding factor. We selected this time as a burn-in to allow for coalescence, to generate diversity and
226 to reach stable allele frequencies. To test for the effect of population size and its changes over time, we

227 simulated ancestral populations pop_A of 10,000, 40,000 and 160,000 individuals, which grossly
228 encompass variation in N_e among great apes, *Peromyscus* and *Mus* (Lack et al. 2010; Phifer-Rixey et al.
229 2012; Prado-Martinez et al. 2013; Harris et al. 2016; Colella et al. 2021) and modeled bottlenecks of
230 different severity associated with the split of pop_A into two daughter populations pop_1 and pop_2 :
231 individuals from pop_A were either sorted into two daughter populations of equal size (N_e in pop_1 and pop_2
232 were $0.5N_e$ of pop_A) or an additional bottleneck further reduced N_e in pop_1 and pop_2 to $0.1N_e$ of pop_A . As
233 our working hypothesis was that chromosome size affects diversity and divergence due to higher
234 recombination rates r in smaller chromosomes, we simulated chromosomes of fixed length (1 Mb) with
235 varying r to account for chromosome size variation, while keeping everything else the same. Assuming
236 one crossover/chromosome on average (Peterson et al. 2019), mean chromosome-wide r was 10^{-8} , so to
237 encompass variation in chromosome size in the mammals examined we simulated nine different
238 recombination rates, spanning $0.33r$ to $3r$, which extends beyond the variation in recombination rates
239 expected to occur in these species based on variation in chromosome size. Note that recombination rates
240 are even across the chromosome and constant through time. We calculated mean gene size (including
241 introns and exons) and mean distance between genes from the gene annotation of the *P. eremicus* genome
242 and built the chromosome structure based on these values, resulting in each chromosome having 9 coding
243 genes of 20.5 kb separated by 94.5 kb of intergenic sequence (Fig. S1B). We used a uniform germline
244 mutation rate as estimated in *M. musculus* (5.7×10^{-9} ; Milholland et al. 2017) across all simulated
245 chromosomes and models. We modeled gene conversion rate ($r/3$) and gene conversion tract length (440
246 bp), when included in the model, based on estimates in *Drosophila melanogaster* (Miller et al. 2016), as
247 no mammal-specific estimates have been established. In neutral models all mutations were neutral,
248 whereas in models with selection mutations in coding genes could be neutral, deleterious or advantageous
249 at a relative frequency of 0.3/1/0.0005, with the non-neutral mutations being always codominant. The
250 fitness effects of the non-neutral mutations were drawn from a gamma distribution with a mean selection
251 coefficient s of $\pm 15.625 \times 10^{-3}$ and a shape parameter alpha of 0.3 based on the parameter space explored
252 by Campos and Charlesworth (2019) and Stankowski et al. (2019). We scaled N_e , μ , and r by a factor of

253 25 to expedite simulations and ran 30 unique simulation replicates for each combination of parameters.
254 All the different parameters used in the simulations are summarized in Table 1. Finally, to validate our
255 assumption that varying recombination rate in lieu of chromosome length recapitulates differences among
256 chromosomes of different lengths, we also simulated three additional chromosomes whose length
257 matched the respective recombination rates. To maintain the proportion of coding sequence constant
258 among chromosomes of fixed and varying length, chromosomes that were longer or shorter than 1 Mb
259 had proportionally more or less coding genes, respectively. We used the 1 Mb chromosome with $1r$ as
260 reference and added a chromosome of 3 Mb with $0.33r$, the lowest recombination rate simulated, a
261 chromosome of 0.33 Mb with $3r$, the highest recombination rate simulation, and a third chromosome of
262 0.66 Mb chromosome with $1.5r$.

263 To investigate the factors affecting levels of diversity in chromosomes of different sizes, we
264 sampled 30 individuals when pop_A reached $20N_e$ generations (i.e. right before the split) for each
265 simulation, output variant sites in a VCF file, and calculated π across the chromosome, in coding genes
266 only, and in intergenic areas only, using VCFtools (Danecek et al. 2011). To obtain estimates of sequence
267 divergence from simulations comparable to those from pairwise alignment of genome assemblies, we
268 calculated d as the proportion of unmatched bases between two haploid genomes sampled randomly from
269 each of the two diverging populations pop_1 and pop_2 . We output these estimates right after the split and
270 every 250,000 generations afterwards, up to 10 million generations. To further disentangle the effect of
271 direct and linked selection, we estimated d also in coding genes and intergenic areas separately between
272 the same genomes sampled above one generation after the split, when d is highest and not affected by
273 decay yet (see Results and discussion). All scripts used in simulations are available at
274 https://github.com/atigano/mammal_chromosome_size/simulations/.

275

276 **Results and discussion**

277 *Empirical data show a strong, inverse relationship between chromosome size and divergence between*
278 *species, with a few exceptions*

279 Chromosome size was a strong significant predictor of mean sequence divergence d in each of the species
280 pairwise comparisons in *Peromyscus* and great apes (all comparisons had $p < 0.001$ using linear models;
281 Fig. 1A and 1C for example comparisons). Chromosome size showed a negative relationship to mean d
282 and explained 62-89% and 46-65% of the variance in mean d across chromosomes (all R^2 are adjusted
283 hereafter) in *Peromyscus* and great apes, respectively. Among *Mus* spp., we found a significant, negative
284 relationship between chromosome size and d only between *M. pahari* and *M. spretus* ($p < 0.001$; Fig. 1E),
285 which explained 42% of the variance in d across chromosomes. We hypothesized that the discrepancy
286 between results from *Mus* and the other two clades examined could be explained by the relatively poor
287 genome structure conservation in *Mus*, so we investigated this further. Among the *Mus* genome
288 alignments, the *M. pahari*/*M. spretus* comparison was the only one where *M. pahari* was used as a
289 reference genome. *M. pahari* is the most divergent (3-6 million years ago) and differs from the other *Mus*
290 species in that it shows a karyotype with 24 chromosomes, while *M. spretus*, *M. musculus* and *M. caroli*
291 exhibit karyotype with only 20 chromosomes (Thybert et al. 2018). Further, fewer synteny breaks
292 between *M. pahari* and the rat (*Rattus norvegicus*) relative the other *Mus* species analyzed here (19 versus
293 35) demonstrate that the *M. pahari* karyotype is the most similar to the ancestral karyotype of the *Mus*
294 species included here (Thybert et al. 2018). As the reference and query genomes in each pairwise
295 comparison were chosen randomly, we produced new alignments and calculated d for all the possible
296 pairwise combinations within each clade to test for the effect of the reference genome to chromosome-
297 level d estimates (Fig. S2, S3, S4). While in the *Peromyscus* and great apes clades all reference-query
298 combinations, including the reciprocal of the comparisons first analyzed (Fig. 1B and 1D) showed a
299 strong negative relationship between chromosome size and d ($R^2 = 0.59-0.91$ among *Peromyscus* and
300 $0.46-0.65$ among great apes, all $p < 0.001$; Fig. S2 and S3), in the *Mus* clade this relationship emerged
301 only when *M. pahari* was used as reference genome ($p < 0.001$; Fig. 1F and S4) and explained 52 and
302 54% of the variance in *M. musculus* and *M. caroli*, respectively (Fig. S4). While a significant positive
303 correlation between neutral human-primate divergence and human recombination rate has been reported
304 at smaller scales (i.e. in 100 kb sliding windows across the genome; Phung et al. 2016), our results show

305 that these relationships between recombination, diversity, and divergence are strong at a large,
306 chromosome scale within three different highly divergent clades (~30-90 MYA), including *Mus*, where, at
307 least in *M. musculus*, the relationship between π and recombination at smaller scales is not always
308 significant (Kartje et al. 2020).

309 The fact that chromosome size in the most ancestral karyotype (*M. pahari*), but not the more
310 derived karyotypes (*M. musculus*, *M. spretus*, and *M. caroli*), is a strong predictor of levels of d between
311 species with different genome structures indicates that these patterns evolve and are maintained across
312 long evolutionary scales. The retention of ancestral patterns suggest that recombination hotspots could be
313 conserved in rearranged chromosomes despite the evolution of a different genome structure, or that a
314 different genomic landscape of recombination has not been sufficient to redistribute variation in sequence
315 divergence expected based on differences in chromosome size over this time scale. In *Heliconius*
316 butterflies, for example, patterns of diversity in fused chromosomes seem to have aligned to expectations
317 based on the size of the derived chromosome size over time, rather than maintaining patterns consistent
318 with the unfused chromosomes of origin (Cicconardi et al. 2021). Though the human genome underwent
319 a chromosomal fusion compared to the other great apes, the correlation between chromosome size and d
320 among great apes did not seem affected by the use of the human genome as reference (i.e. chromosome
321 size did not explain a lower proportion of the variance in these comparisons; Fig. 1C, 1D, S3).

322 The choice of a model species is largely based on its potential to provide insights that are
323 generalizable to other organisms, yet our results builds on previous work in *M. musculus* (Jensen-Seaman
324 et al. 2004; Kartje et al. 2020) showing that the *Mus* clade is rather an outlier, and does not serve as a
325 good model to analyze general patterns with regards to how genome and chromosome structure affect and
326 shape heterogenous levels and patterns of diversity and divergence across the genome. However, our
327 analysis of the *Mus* genomes provides insight into the reasons a species may deviate from expectations,
328 showing that the dramatic chromosomal rearrangements occurred in the *Mus* clade seem to explain the
329 apparent lack of a relationship between chromosome size and recombination rate, π , and d when a derived
330 karyotype is used as reference. Moreover, the lower proportion of the variation in d explained in *Mus*

331 compared to the other two clades, even when the ancestral karyotype of *M. pahari* is used as reference,
332 may be due to an ongoing shift towards expectations based on the size of the rearranged chromosomes, as
333 suggested in *Heliconius* butterflies (Cicconardi et al. 2021).

334 Another factor that might explain variation among clades in the strength of the association
335 between chromosome size and divergence (Fig. 1) is gene flow and introgression. Introgression can
336 increase diversity within species and decrease divergence between hybridizing species (Tigano and
337 Friesen 2016); and the distribution and length of introgressed sequence from one species to another is
338 determined by the interplay of selection and recombination (Duranton et al. 2018). It is therefore plausible
339 that chromosomes of different sizes could affect the fate of introgressed DNA, in terms of both the
340 distribution and length of donor sequence. Inversely, the heterogeneous landscape of introgression could
341 affect the power of chromosome size in explaining variation in diversity and divergence across
342 chromosomes. The adaptive introgression of a rodenticide-resistant allele from *Mus spretus* to *M.*
343 *musculus* shows that the fitness benefit of a beneficial donor allele can overcome incomplete reproductive
344 barriers between species (Song et al. 2011). Moreover, the reticulate evolution of primates, and possibly
345 many other understudied clades, support the occurrence of ancient gene flow and introgression among
346 many extant and extinct taxa during and post-speciation (Feder et al. 2012; Vanderpool et al. 2020).
347 However, although gene flow between these and with other unsampled species cannot be excluded,
348 hybridization is rare among *Peromyscus* species (e.g., Barko and Feldhamer 2002; Leo and Millien 2017);
349 hybrid sterility or infertility in *Mus* has been reported between species (Dejager et al. 2009) and even
350 between *M. musculus* subspecies (Turner et al. 2011); and among great apes recent hybridization appears
351 limited to intraspecific gene flow (Fontseré et al. 2019). Therefore, gene flow does not seem to affect the
352 relationship between chromosome size and divergence among the species included in this study, though is
353 a factor to consider when comparing species connected by historical or contemporary gene flow.

354

355

356

357 *Evolutionary simulations reveal the factors driving the empirical patterns.*

358 Simulations helped generate a mechanistic understanding of most of the empirical patterns reported in this
359 and other studies (Dutoit et al. 2017; Murray et al. 2017; Kartje et al. 2020; Tigano et al. 2020). Patterns
360 of diversity observed across simulated chromosomes that varied in recombination rate only were
361 qualitatively equivalent to the simulated chromosomes that varied also in length (Fig. S6), showing that,
362 as long as all the other parameters are constant and uniform across the chromosomes, including mutation
363 rate and proportion of coding genes, variation in recombination rate alone suffices to recapitulate
364 variation in chromosome length. Therefore, here we show and discuss results based on simulated
365 chromosomes that vary in recombination rate only. In neutral simulations, we did not observe variation in
366 π among chromosomes with different recombination rates whether the model included gene conversion or
367 not (ANOVA, $p > 0.05$). These results indicate that recombination alone does not explain variation in π
368 among chromosomes and that gene conversion does not contribute substantially to increasing levels of π ,
369 at least at the rates that we assumed and over relatively short evolutionary times ($20N_e$ generations). Gene
370 conversion occurs at a fraction of the recombination rate and affects only a small segment of DNA (100-
371 2000 bp) at a time (Korunes and Noor 2017; Korunes and Noor 2019), hence its effect on chromosome-
372 wide levels of π may be detectable only over long evolutionary times. Recombination could also be
373 mutagenic *per se* by promoting *de novo* mutations at the DNA breaks caused by crossovers, but the
374 mechanism underlying this phenomenon is not clear (Hodgkinson and Eyre-Walker 2011). We did not
375 model crossover mutagenesis in our simulations, but a recent study in humans found the mutation rate
376 associated with crossovers to be ~4%, i.e. one *de novo* mutation every ~23 crossovers (Halldorsson et al.
377 2019) suggesting that crossover mutagenesis could contribute to, but not entirely account for, the
378 variation in π among chromosomes of different sizes over long evolutionary times, similar to gene
379 conversion. In contrast, in models with selection, recombination rate was a significant ($p < 0.001$)
380 predictor of differences in π among chromosomes across populations of three vastly different N_e (Fig.
381 2A). However, $\Delta\pi$ - the difference in π between the chromosomes with the highest and lowest
382 recombination rates - spanned over two orders of magnitude when comparing the smallest and the largest

383 simulated ancestral populations ($\Delta\pi = 3.16 \cdot 10^{-5} - 2.69 \cdot 10^{-3}$; Fig. 3). Also the proportions of variance in π
384 explained by recombination rate increased with N_e : they were 13, 60, and 85% in populations of 10,000,
385 40,000 and 160,000 individuals respectively in models without gene conversion (estimates were similar
386 for models with gene conversion, except for the smallest N_e where r explained 27% of the variation),
387 suggesting that while selection is the main determinant of the relationship between recombination and π
388 in large populations, genetic drift prevails in smaller populations.

389 The comparison of π across models with and without selection shows that diversity is lower
390 overall, regardless of the recombination rate, in chromosomes affected by selection (Fig. 2A). The
391 reduction in π is strongest at the coding genes, which experience both positive and negative selection
392 directly, and indirectly through linked selection (Fig. 2A). Chromosome-wide estimates are more similar
393 to those based on the analysis of intergenic areas subjected to linked selection only (Fig. 2A), which is at
394 least partly due to the relatively much larger proportion of non-coding over coding regions. Nonetheless,
395 a positive relationship between recombination rate and π is evident across the different genomic areas and
396 N_e considered (Fig. 2A). The comparison of π estimates from across the chromosome, coding genes only,
397 and intergenic areas only, corroborates that differences in diversity among chromosomes of different sizes
398 are due to the balance between selection and recombination, with selection reducing diversity and
399 recombination reducing linkage disequilibrium, which in turn reduces the effect of linked selection. As
400 recombination increases, it more strongly counteracts linked selection in the intergenic areas, to the point
401 of almost restoring levels of diversity like those expected under a neutral model (Fig. 2A). In other words,
402 in our simulations the interplay between recombination and selection is the main factor driving the
403 inverse correlation between chromosome size and π , a pattern that is described in many species.

404 The fact that recombination was a stronger contributor to variation in π in larger populations than
405 in smaller ones could be due to one or the combination of two factors: 1) as the effect of selection in the
406 genome depends on both effective population size and the strength of selection ($N_e s$), larger populations
407 will have proportionally more selective sweeps than smaller populations - because more mutations in
408 small populations will have scaled coefficients so small that they will actually behave as neutral - and

409 these sweeps will be more strong and efficient at removing diversity, and 2) larger populations will have
410 higher population recombination rates ($\rho = 4N_e r$), which will break linkage disequilibrium even more
411 efficiently in chromosomes with high recombination rates. As smaller population will have proportionally
412 more mutations behaving as neutral ones, more mutations will be more predominantly governed by
413 stochasticity rather than by the deterministic effect of selection in these small populations (Charlesworth
414 2009), which is consistent with selection explaining less variation in π in smaller populations than in
415 larger ones (see above).

416 In neutral models, d did not vary across chromosomes with different recombination rates
417 (ANOVA, $p \gg 0.05$; Fig. 3B), while in models with selection differences in d among chromosomes one
418 generation after the split were significantly different from zero (ANOVA, $p < 0.001$; Fig. 2B) and
419 strongly correlated with recombination rate ($p < 0.001$; Fig. 2B), i.e. chromosomes with lower
420 recombination rates had lower d between populations, across all three simulated values of N_e . Sequence
421 divergence right after the split reflected the levels of diversity within the ancestral population before the
422 split across all models, with higher Δd - the difference in d between the chromosomes with the highest
423 and lowest recombination rates - in larger populations (Fig. 2B). Similar to the patterns observed for π , d
424 was lowest in coding regions and highest in intergenic areas, with chromosome-wide estimates lower
425 than, but similar to, the latter (Fig. 2B). Testing empirically whether species with higher ancestral N_e
426 show higher Δd would support the contribution of demography in the relationship between recombination
427 and d . However, across the three clades examined here, N_e and divergence times between species seem to
428 covary, for example with great apes having not only the smallest N_e but also the most recent species
429 divergence, so that the actual relative contributions of N_e and divergence times cannot be disentangled
430 using empirical data in this study.

431 In neutral models, d increases linearly with time ($4N_e\mu + 2T\mu$, where T is the number of
432 generations) so the severity of the bottleneck at the time of the split does not have any effect on
433 divergence between isolated populations in our neutral simulations, even at the smallest N_e . Although
434 genetic drift was *de facto* the only evolutionary force driving changes in allele frequency in these neutral

435 models, its effect size ($= 1/2N_e$) in our simulated populations was nonetheless very small ($6.25 \cdot 10^{-6} - 10^{-4}$), which indicates that new mutations are the main source of d over time in neutral models. In fact, our d
436 estimates encompass both fixed and segregating mutations in each of the two compared populations.
437

438 In models with selection, d increased over time, though at a slower pace than in neutral models,
439 and faster in smaller populations relative to larger populations (Fig. 3). Further, while larger populations
440 showed higher overall divergence than smaller ones in the early stages of divergence, the trend reversed
441 with time: after 10 million generations d between the smallest populations ($N_e = 5,000$ individuals each)
442 surpassed d both between the medium-sized ($N_e = 20,000$ individuals each) and between the largest
443 populations ($N_e = 80,000$ individuals each; Fig. 3). This pattern was even more pronounced when
444 populations pop_1 and pop_2 were affected by a stronger bottleneck at the time of the split from pop_A :
445 populations of all sizes accumulated d faster than in the models with a weaker bottleneck, and even faster
446 between the smallest populations ($N_e = 1,000$ individuals each) compared to estimates from larger
447 populations ($N_e = 4,000$ and $16,000$ individuals each, respectively; Fig. S5). These results show how
448 genetic drift is much stronger in small populations, but only in the models with selection (Fig. S5).
449 Neutral mutations fix at a much faster rate than those under selection because the fixation probability of a
450 locus under selection depends also on the strength of selection acting on its linked sites (Hill-Robertson
451 interference; Hill and Robertson 1966; Felsenstein 1974). Given the distribution of fitness effects (DFE)
452 we simulated, the probability of a beneficial mutation to effectively act as a neutral mutation (i.e. that $N_e s$
453 < 1) is higher in smaller populations than in larger ones (Charlesworth 2009). Therefore, in smaller
454 population, a higher proportion of beneficial or deleterious mutations will act as neutral and their fixation
455 probability will be higher and depend only on the combination of genetic drift and linked selection, which
456 in turn will depend on the strength of selection acting on the linked mutation and the rate of
457 recombination affecting linkage disequilibrium between the two mutations.

458 We found that Δd decreased with divergence time in all models with selection (Fig. 4), suggesting
459 that either divergence rate is relatively accelerated in large chromosomes or slowed down in small ones.
460 Based on what discussed above, larger chromosomes, where recombination rates are lower, should

461 experience stronger Hill-Robertson interference, and hence lower fixation probabilities and slower
462 divergence rate, which is in contrast with what observed. Alternatively, lower recombination in larger
463 chromosomes could strengthen the effect of linked selection, resulting in local chromosome-wide
464 reductions in N_e , and thus stronger genetic drift and faster rate of sequence divergence than smaller
465 chromosomes with higher recombination rates. This is clearly illustrated by an empirical study on
466 Bornean and Sumatran Orangutans (*P. pygmaeus* and *P. abelii*) showing that estimates of ancestral N_e
467 vary among chromosomes and that chromosome size is a strong predictor of variation in both inferred
468 ancestral N_e and recombination rate, which in turn suggests a direct relationship between these two
469 (Mailund et al. 2011). Additionally, Phung et al. (2016) showed that the window-based correlation
470 between recombination and divergence rate in simulated genomes decreased with splitting time, and
471 attributed this decrease to a concurrent decrease in levels of ancestral variation. At the chromosome level,
472 these observations suggest that chromosomes of different sizes may lose ancestral variation at different
473 rates and thus may account for the decay in Δd .

474 These different rates of divergence explain why over time Δd becomes negative in our
475 simulations, i.e. the chromosome with the lowest recombination rate becomes more divergent than the
476 chromosome with the highest recombination rate, in the populations with the smaller N_e (Fig. 4). Initially,
477 the differences in Δd will be determined by $\Delta\pi$ in the ancestral population at the time of the split, but with
478 time the different divergence rates among chromosomes caused by the interplay of recombination,
479 selection, and thus drift, will erode Δd , and even reverse it (Fig. 4). Furthermore, the severity of the
480 bottleneck at the species split affected the Δd decay rate, with a faster decay in less severely reduced N_e ,
481 regardless of ancestral N_e (Fig. 4). Also gene conversion seemed to accelerate the Δd decay overall, but
482 not in the largest population experiencing the weaker bottleneck (Fig. 4). That Δd decay was generally
483 faster both in populations experiencing milder bottlenecks, which therefore had larger N_e , and in models
484 with gene conversion compared to those without, suggests that higher mutation rates in these cases can
485 accelerate Δd decay. Although the ultimate mechanism is not clear, faster Δd decay may be explained by
486 the rate of loss of ancestral polymorphism (Phung et al. 2016), which should be higher with higher

487 mutation rates. Importantly, the effect of gene conversion becomes more evident after 5 million
488 generations (Fig. 4), showing that, although gene conversion is not the main determinant of differences in
489 π and d among chromosomes of different sizes, it can contribute to these patterns over long evolutionary
490 times. The evolutionary simulations provide clear insights into why the variation in divergence among
491 chromosomes of different sizes decreases with time, and suggest that it would require either small N_e
492 and/or long divergence times to observe a negative Δd . We did not observe any negative Δd in our species
493 pairwise comparisons. In the future, the empirical test of these observations will require the inclusion of
494 additional clades and larger number of species comparisons within clades to verify how commonly this
495 occurs empirically and to disentangle the factors promoting, or hindering, this pattern.

496 Our simulations were based on reasonably realistic parameters, except for the absence of
497 neutrally evolving introns in simulated genes, to reach an acceptable compromise between capturing the
498 complexity of the evolutionary processes, and their interactions, while maintaining enough statistical
499 power to understand the relative roles of the many factors at play. Notwithstanding that empirically-
500 derived values for the factors included in our simulations are not available for most species or are difficult
501 to accurately estimate, excluding introns provided more target sequence for selection to act on and a good
502 trade-off in terms of computational time and resources. With the exception of a clear effect of N_e and
503 divergence time in the magnitude of the variation in d observed among chromosomes, our evolutionary
504 simulations well illustrate the processes driving the empirical patterns of divergence between species
505 described in three different clades of mammals: in the absence of chromosomal rearrangements, the
506 interplay of recombination and selection determines levels of π in the ancestral species; higher π in the
507 ancestral species results in higher d among haplotypes sorted into the daughter species, thus explaining
508 the differences in π and d among chromosomes of different sizes.

509

510 *Empirical analyses and simulations highlight the rule and the exceptions*

511 Species showing an inverse relationship between recombination rate and chromosome size are found
512 among mammals, birds, yeast, worms, and plants (Pessia et al. 2012), which highlights that this

513 relationship is not an idiosyncratic feature of a particular taxon but rather a widespread feature of genome
514 evolution. Our evolutionary simulations show that varying recombination rates across chromosomes
515 should result in differences in π and d among chromosomes of different sizes, but empirical support for
516 this prediction is mixed. In *M. musculus*, for example, chromosome size is not a good predictor of
517 variation in π within the species (Pessia et al. 2012) or d to other *Mus* spp. (our study). Our analyses here
518 have shown that this lack of correlation is likely due to dramatic changes in the genome structure of *M.*
519 *musculus* and other congeneric species relative to their common ancestor (most similar to *M. pahari*).
520 Future work, including additional species comparisons and evolutionary simulations, will focus on testing
521 the role of chromosomal rearrangement in the presence of a relationship between chromosome size and
522 divergence across species and over time. These results also stress the importance of the choice of the
523 reference genome in this type of analysis. Not only does the reference genome potentially mask existing
524 relationships due to the evolution of different genome structure, as we have shown here, but also its
525 quality is crucial to obtain high-quality genome alignments, to calculate d accurately, and to estimate
526 chromosome sizes from sequence length in the absence of cytological data.

527 No significant relationship between chromosome size and divergence between human and
528 chimpanzee was found in another study (Patterson et al. 2006), but these results were based on only 20
529 Mb of aligned sequences. Moreover, different avian species have shown a positive (Dutoit et al. 2017), a
530 negative (Manthey et al. 2015), or no relationship (Callicrate et al. 2014) between chromosome size and
531 π . Dramatic chromosomal rearrangements can be excluded in these examples (Ellegren 2010), begging
532 the question: what other factors could explain these deviations from our model? First, given the variation
533 in d within chromosomes, incomplete genome sampling may confound these chromosome-level
534 relationships. Second, Dutoit and colleagues (2017) argue that in the collared flycatcher (*Ficedula*
535 *albicollis*) a positive relationship between chromosome size and π , which is opposite to expectations,
536 could be explained by the density of targets of selection, higher in smaller chromosomes than in larger
537 ones in this species. However, given the high degree of synteny conservation among birds (Ellegren
538 2010), all avian species should show a similar pattern, which is not the case. For example, the comparison

539 of genome-wide patterns in π in the passenger pigeon (*Ectopistes migratorius*), known as the most
540 abundant bird in North America before it went extinct, and the band-tailed pigeon (*Patagioenas fasciata*),
541 with a current population size three orders of magnitude smaller, not only shows higher π in smaller
542 chromosomes in both species, but also the effect of N_e on $\Delta\pi$, as per our predictions (Murray et al. 2017).
543 Our analyses highlight the contribution of demography (i.e. N_e , severity of bottleneck and genetic drift) in
544 affecting, and even reversing, the relationship between recombination, π , and d , which could potentially
545 explain the opposite correlation reported in the collared flycatcher. The importance of historical
546 demography has been demonstrated also in the divergence of the sex chromosome Z in *Heliconius*
547 butterflies using a combination of empirical data and evolutionary simulations (Van Belleghem et al.
548 2018). Alternatively, the strength of selection, rather than the density of targets of selection, could disrupt
549 the correlation between chromosome size and π in case of strong selective sweeps preferentially occurring
550 in small chromosomes. Finally, limited variation in recombination, π , and d among chromosomes could
551 be simply due to lack of variation in chromosome size. The analysis of 128 eukaryotic and prokaryotic
552 genomes has shown that variation in chromosome size is directly proportional to genome size (Li et al.
553 2011), suggesting that variation in recombination, π , and d among chromosomes should decrease with
554 genome size.

555

556 *Conclusions*

557 Variation in recombination across the genome affects the evolution and maintenance of traits relevant to
558 adaptation and speciation, the genomic architecture of the loci underlying those traits, and our ability to
559 detect those loci (Yeaman and Otto 2011; Yeaman 2013; Cruickshank and Hahn 2014; Burri et al. 2015;
560 Roesti 2018; Lotterhos 2019; Booker et al. 2020). Heterogenous recombination rates can also lead to the
561 inference of different demographic histories and ancestral N_e estimates depending on the chromosome or
562 region of chromosome analyzed (Mailund et al. 2011; Robinson et al. 2021). We have shown strong
563 evidence from empirical analyses and evolutionary simulations that the inverse relationship between
564 recombination rate and chromosome size can result in significant differences in π and d among

565 chromosomes of different sizes, indicating that variation in recombination rates among chromosomes of
566 different sizes has an overall stronger effect than variation in recombination rates within chromosomes.

567 In the clades included in this study, N_e covaries with divergence time scales, thus it is not possible
568 to disentangle the relative effect of these two factors on patterns of divergence at this time. Furthermore,
569 we cannot currently demonstrate that the chromosomal rearrangements in the *Mus* clade have a causal
570 effect on masking the ancestral patterns of divergence, but nonetheless show a strong correlation. Future
571 analyses of species and clades with different combinations of N_e , divergence times, and degree of genome
572 structure conservation will help address these gaps. Nonetheless, our study shows that chromosome size
573 should be considered in the study of the genomic basis of adaptation and speciation. Do smaller
574 chromosomes play a proportionally more prominent role than larger chromosomes in adaptation and
575 speciation? Or are these differences in π and d strong enough to confound signals of selection in the
576 genome? As chromosome-level assemblies and population whole genome resequencing data of closely-
577 related species become available for an increasing number of taxa, the combination of empirical and
578 theoretical investigations will help address these outstanding questions and generate new ones on
579 chromosome and genome evolution.

580 **References**

- 581 Arbeithuber B, Betancourt AJ, Ebner T, Tiemann-Boege I. 2015. Crossovers are associated with mutation
582 and biased gene conversion at recombination hotspots. *Proc. Natl. Acad. Sci. U. S. A.* 112:2109–
583 2114.
- 584 Begun DJ, Aquadro CF. 1992. Levels of naturally occurring DNA polymorphism correlate with
585 recombination rates in *D. melanogaster*. *Nature* 356:519–520.
- 586 Birky CW Jr, Walsh JB. 1988. Effects of linkage on rates of molecular evolution. *Proc. Natl. Acad. Sci.*
587 *U. S. A.* 85:6414–6418.
- 588 Booker TR, Yeaman S, Whitlock M. 2020. Variation in recombination rate affects detection of outliers in
589 genome scans under neutrality. *Mol. Ecol.* 29:4274-4279.
- 590 Burri R, Nater A, Kawakami T, Mugal CF, Olason PI, Smeds L, Suh A, Dutoit L, Bureš S, Garamszegi
591 LZ, et al. 2015. Linked selection and recombination rate variation drive the evolution of the genomic
592 landscape of differentiation across the speciation continuum of *Ficedula* flycatchers. *Genome Res.*
593 25:1656–1665.
- 594 Butlin RK. 2005. Recombination and speciation. *Mol. Ecol.* 14:2621–2635.
- 595 Callicrate T, Dikow R, Thomas JW, Mullikin JC, Jarvis ED, Fleischer RC, NISC Comparative
596 Sequencing Program. 2014. Genomic resources for the endangered Hawaiian honeycreepers. *BMC*
597 *Genomics* 15:1098.
- 598 Campos JL, Charlesworth B. 2019. The Effects on Neutral Variability of Recurrent Selective Sweeps and
599 Background Selection. *Genetics* 212:287–303.
- 600 Cicconardi F, Lewis JJ, Martin S, Reed RD, Danko CG., & Montgomery, S. H. (2021). Chromosome
601 fusion affects genetic diversity and evolutionary turnover of functional loci but consistently depends
602 on chromosome size. *Mol. Biol. Evol.* <https://doi.org/10.1093/molbev/msab185>
- 603 Charlesworth B. 2009. Effective population size and patterns of molecular evolution and variation. *Nat.*
604 *Rev. Genet.* 10:195–205.
- 605 Colella JP, Tigano A, MacManes MD. 2020. A linked-read approach to museomics: Higher quality de
606 novo genome assemblies from degraded tissues. *Mol Ecol Res*, 20:856-870.
- 607 Colella JP, Tigano A, Dudchenko O, Omer AD, Khan R, Bochkov ID, Aiden EL, MacManes MD. 2021.
608 Limited evidence for parallel evolution among desert-adapted *Peromyscus* deer mice. *J. Hered.*
609 112:286-302.
- 610 Coop G, Przeworski M. 2007. An evolutionary view of human recombination. *Nat. Rev. Genet.* 8:23–34.
- 611 Cruickshank TE, Hahn MW. 2014. Reanalysis suggests that genomic islands of speciation are due to
612 reduced diversity, not reduced gene flow. *Mol. Ecol.* 23:3133–3157.
- 613 Cutter AD, Choi JY. 2010. Natural selection shapes nucleotide polymorphism across the genome of the
614 nematode *Caenorhabditis briggsae*. *Genome Res.* 20:1103–1111.
- 615 Danecsek P, Auton A, Abecasis G, Albers CA, Banks E, DePristo MA, Handsaker RE, Lunter G, Marth

- 616 GT, Sherry ST, et al. 2011. The variant call format and VCFtools. *Bioinformatics* 27:2156–2158.
- 617 Delmore KE, Lugo Ramos JS, Van Doren BM, Lundberg M, Bensch S, Irwin DE, Liedvogel M. 2018.
618 Comparative analysis examining patterns of genomic differentiation across multiple episodes of
619 population divergence in birds. *Evol. Lett.* 2:76–87.
- 620 Dion-Côté A-M, Symonová R, Lamaze FC, Pelikánová Š, Ráb P, Bernatchez L. 2017. Standing
621 chromosomal variation in Lake Whitefish species pairs: The role of historical contingency and
622 relevance for speciation. *Mol. Ecol.* 26:178–192.
- 623 Dudchenko O, Batra SS, Omer AD, Nyquist SK, Hoeger M, Durand NC, Shamim MS, Machol I, Lander
624 ES, Aiden AP, et al. 2017. De novo assembly of the *Aedes aegypti* genome using Hi-C yields
625 chromosome-length scaffolds. *Science* 356:92–95.
- 626 Dudchenko O, Shamim MS, Batra SS, Durand NC, Musial NT, Mostofa R, Pham M, St Hilaire BG, Yao
627 W, Stamenova E, et al. 2018. The Juicebox Assembly Tools module facilitates de novo assembly of
628 mammalian genomes with chromosome-length scaffolds for under \$1000. Available from:
629 <http://dx.doi.org/10.1101/254797>
- 630 Durand NC, Robinson JT, Shamim MS, Machol I, Mesirov JP, Lander ES, Aiden EL. 2016. Juicebox
631 Provides a Visualization System for Hi-C Contact Maps with Unlimited Zoom. *Cell Syst* 3:99–101.
- 632 Duranton M, Allal F, Fraïsse C, Bierne N, Bonhomme F, Gagnaire PA. 2018. The origin and remodeling
633 of genomic islands of differentiation in the European sea bass. *Nature Comm.*, 9: 1-11.
- 634 Dutoit L, Burri R, Nater A, Mugal CF, Ellegren H. 2017. Genomic distribution and estimation of
635 nucleotide diversity in natural populations: perspectives from the collared flycatcher (*Ficedula*
636 *albicollis*) genome. *Mol. Ecol. Resour.* 17:586–597.
- 637 Ellegren H. 2010. Evolutionary stasis: the stable chromosomes of birds. *Trends Ecol. Evol.* 25:283–291.
- 638 Ellegren H, Galtier N. 2016. Determinants of genetic diversity. *Nat. Rev. Genet.* 17:422–433.
- 639 Farré M, Micheletti D, Ruiz-Herrera A. 2013. Recombination Rates and Genomic Shuffling in Human
640 and Chimpanzee—A New Twist in the Chromosomal Speciation Theory. *Mol. Biol. Evol.* 30:853–
641 864.
- 642 Felsenstein J. 1974. The evolutionary advantage of recombination. *Genetics* 78:737–756.
- 643 Gilbert KJ, Pouyet F, Excoffier L, Peischl S. 2020. Transition from Background Selection to Associative
644 Overdominance Promotes Diversity in Regions of Low Recombination. *Curr. Biol.* 30:101–107.e3.
- 645 Graphodatsky AS, Trifonov VA, Stanyon R. 2011. The genome diversity and karyotype evolution of
646 mammals. *Mol. Cytogenet.* 4:22.
- 647 Haenel Q, Laurentino TG, Roesti M, Berner D. 2018. Meta-analysis of chromosome-scale crossover rate
648 variation in eukaryotes and its significance to evolutionary genomics. *Mol. Ecol.* 27:2477–2497.
- 649 Halldorsson BV, Palsson G, Stefansson OA, Jonsson H, Hardarson MT, Eggertsson HP, Gunnarsson B,
650 Oddsson A, Halldorsson GH, Zink F, et al. 2019. Characterizing mutagenic effects of recombination
651 through a sequence-level genetic map. *Science* [Internet] 363. Available from:
652 <http://dx.doi.org/10.1126/science.aau1043>

- 653 Haller BC, Messer PW. 2019. SLiM 3: Forward Genetic Simulations Beyond the Wright–Fisher Model.
654 *Mol. Biol. Evol.* 36:632–637.
- 655 Harris SE, Xue AT, Alvarado-Serrano D, Boehm JT, Joseph T, Hickerson MJ, Munshi-South J. 2016.
656 Urbanization shapes the demographic history of a native rodent (the white-footed mouse,
657 *Peromyscus leucopus*) in New York City. *Biology Letters* [Internet] 12:20150983. Available from:
658 <http://dx.doi.org/10.1098/rsbl.2015.0983>
- 659 Hassold T, Hunt P. 2001. To err (meiotically) is human: the genesis of human aneuploidy. *Nat. Rev.*
660 *Genet.* 2:280–291.
- 661 Hauffe HC, Searle JB. 1993. Extreme karyotypic variation in a *Mus musculus domesticus* hybrid zone:
662 the tobacco mouse story revisited. *Evolution* 47:1374–1395.
- 663 Hellmann I, Ebersberger I, Ptak SE, Pääbo S, Przeworski M. 2003. A neutral explanation for the
664 correlation of diversity with recombination rates in humans. *Am. J. Hum. Genet.* 72:1527–1535.
- 665 Henderson EC, Brelsford A. 2020. Genomic differentiation across the speciation continuum in three
666 hummingbird species pairs. *BMC Evol. Biol.* 20:113.
- 667 Hill WG, Robertson A. 1966. The effect of linkage on limits to artificial selection. *Genetical Research*
668 [Internet] 8:269–294. Available from: <http://dx.doi.org/10.1017/s0016672300010156>
- 669 Hodgkinson A, Eyre-Walker A. 2011. Variation in the mutation rate across mammalian genomes. *Nat.*
670 *Rev. Genet.* 12:756–766.
- 671 Hudson RR, Kaplan NL. 1995. Deleterious background selection with recombination. *Genetics*
672 141:1605–1617.
- 673 Jensen-Seaman MI, Furey TS, Payseur BA, Lu Y, Roskin KM, Chen C-F, Thomas MA, Haussler D,
674 Jacob HJ. 2004. Comparative recombination rates in the rat, mouse, and human genomes. *Genome*
675 *Res.* 14:528–538.
- 676 Kaback DB, Guacci V, Barber D, Mahon JW. 1992. Chromosome size-dependent control of meiotic
677 recombination. *Science* 256:228–232.
- 678 Kartje ME, Jing P, Payseur BA. 2020. Weak Correlation between Nucleotide Variation and
679 Recombination Rate across the House Mouse Genome. *Genome Biol. Evol.* 12:293–299.
- 680 Kawakami T, Smeds L, Backström N, Husby A, Qvarnström A, Mugal CF, Olason P, Ellegren H. 2014.
681 A high-density linkage map enables a second-generation collared flycatcher genome assembly and
682 reveals the patterns of avian recombination rate variation and chromosomal evolution. *Molecular*
683 *Ecology* [Internet] 23:4035–4058. Available from: <http://dx.doi.org/10.1111/mec.12810>
- 684 Korunes KL, Noor MAF. 2017. Gene conversion and linkage: effects on genome evolution and
685 speciation. *Mol. Ecol.* 26:351–364.
- 686 Korunes KL, Noor MAF. 2019. Pervasive gene conversion in chromosomal inversion heterozygotes. *Mol.*
687 *Ecol.* 28:1302–1315.
- 688 Lack JB, Pfau RS, Wilson GM. 2010. Demographic history and incomplete lineage sorting obscure
689 population genetic structure of the Texas mouse (*Peromyscus attwateri*). *J. Mammal.* 91:314–325.

- 690 Li X, Zhu C, Lin Z, Wu Y, Zhang D, Bai G, Song W, Ma J, Muehlbauer GJ, Scanlon MJ, et al. 2011.
691 Chromosome size in diploid eukaryotic species centers on the average length with a conserved
692 boundary. *Mol. Biol. Evol.* 28:1901–1911.
- 693 Lotterhos KE. 2019. The Effect of Neutral Recombination Variation on Genome Scans for Selection. *G3*
694 9:1851–1867.
- 695 Mailund T, Dutheil JY, Hobolth A, Lunter G, Schierup MH. 2011. Estimating divergence time and
696 ancestral effective population size of Bornean and Sumatran orangutan subspecies using a coalescent
697 hidden Markov model. *PLoS Genet.* 7:e1001319.
- 698 Manthey JD, Klicka J, Spellman GM. 2015. Chromosomal patterns of diversity and differentiation in
699 creepers: a next-gen phylogeographic investigation of *Certhia americana*. *Heredity* 115:165–172.
- 700 Marçais G, Delcher AL, Phillippy AM, Coston R, Salzberg SL, Zimin A. 2018. MUMmer4: A fast and
701 versatile genome alignment system. *PLoS Comput. Biol.* 14:e1005944.
- 702 Mather K. 1938. Crossing-over. *Biol. Rev. Camb. Philos. Soc.* 13:252–292.
- 703 Milholland B, Dong X, Zhang L, Hao X, Suh Y, Vijg J. 2017. Differences between germline and somatic
704 mutation rates in humans and mice. *Nat. Commun.* 8:15183.
- 705 Miller DE, Smith CB, Kazemi NY, Cockrell AJ, Arvanitakis AV, Blumenstiel JP, Jaspersen SL, Hawley
706 RS. 2016. Whole-Genome Analysis of Individual Meiotic Events in *Drosophila melanogaster*
707 Reveals That Noncrossover Gene Conversions Are Insensitive to Interference and the Centromere
708 Effect. *Genetics* 203:159–171.
- 709 Moura MN, Cardoso DC, Lima Baldez BC. 2020. Intraspecific variation in the karyotype length and
710 genome size of fungus-farming ants (genus *Mycetophylax*), with remarks on procedures for the
711 estimation of genome size in the Formicidae by flow cytometry. *PLoS One* [Internet]. Available
712 from: <https://journals.plos.org/plosone/article?id=10.1371/journal.pone.0237157>
- 713 Murray GGR, Soares AER, Novak BJ, Schaefer NK, Cahill JA, Baker AJ, Demboski JR, Doll A, Da
714 Fonseca RR, Fulton TL, et al. 2017. Natural selection shaped the rise and fall of passenger pigeon
715 genomic diversity. *Science* 358:951–954.
- 716 Nachman MW. 2001. Single nucleotide polymorphisms and recombination rate in humans. *Trends Genet.*
717 17:481–485.
- 718 Ohta T. 1971. Associative overdominance caused by linked detrimental mutations. *Genet. Res.* 18:277–
719 286.
- 720 Patterson N, Richter DJ, Gnerre S, Lander ES, Reich D. 2006. Genetic evidence for complex speciation of
721 humans and chimpanzees. *Nature* 441:1103–1108.
- 722 Pessia E, Popa A, Mousset S, Rezvoy C, Duret L, Marais GAB. 2012. Evidence for widespread GC-
723 biased gene conversion in eukaryotes. *Genome Biol. Evol.* 4:675–682.
- 724 Peterson AL, Miller ND, Payseur BA. 2019. Conservation of the genome-wide recombination rate in
725 white-footed mice. *Heredity* 123:442–457.
- 726 Phifer-Rixey M, Bonhomme F, Boursot P, Churchill GA, Piálek J, Tucker PK, Nachman MW. 2012.
727 Adaptive evolution and effective population size in wild house mice. *Mol. Biol. Evol.* 29:2949–2955.

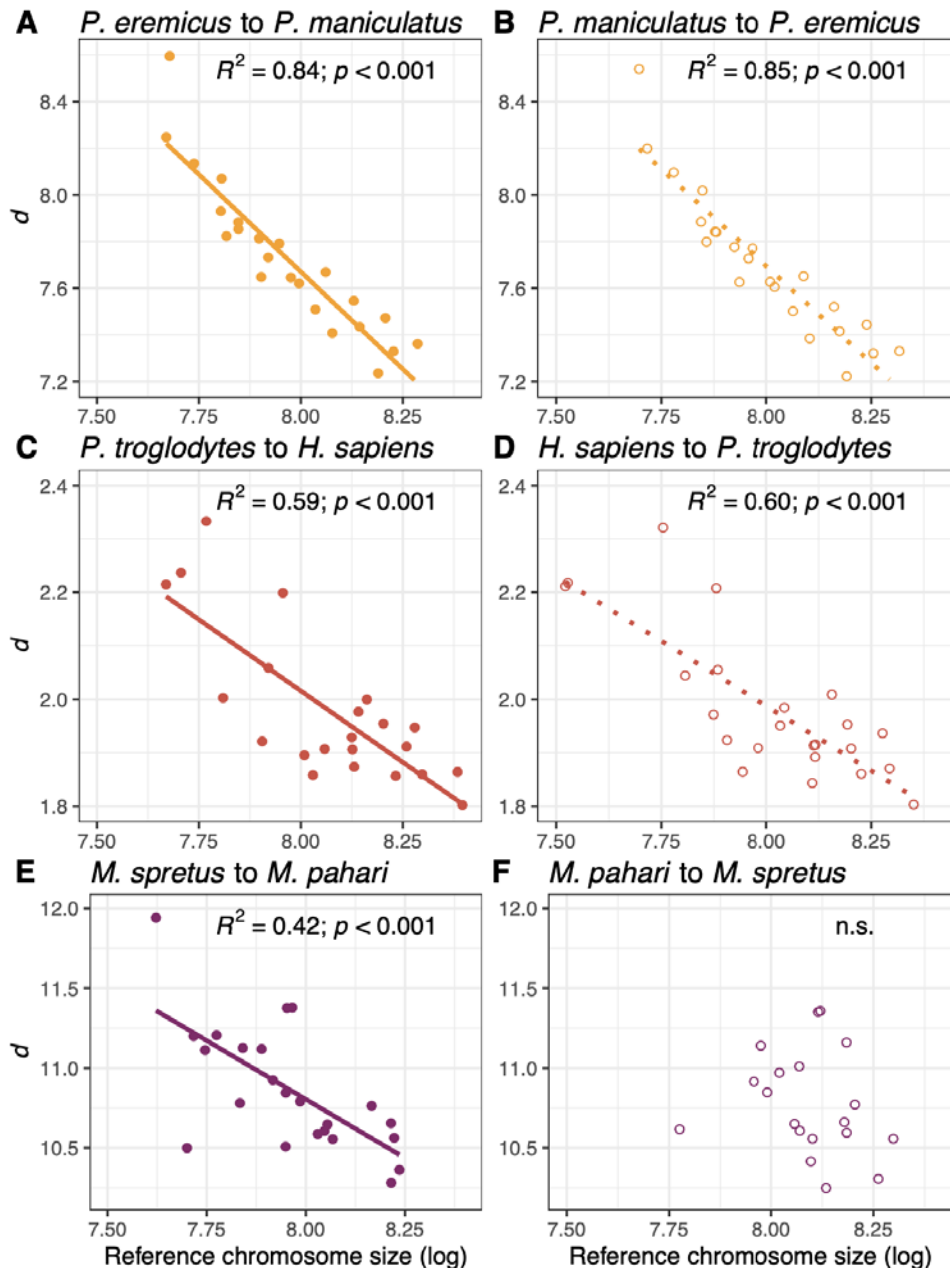
- 728 Phung TN, Huber CD, Lohmueller KE. 2016. Determining the Effect of Natural Selection on Linked
729 Neutral Divergence across Species. *PLoS Genet.* 12:e1006199.
- 730 Prado-Martinez J, Sudmant PH, Kidd JM, Li H, Kelley JL, Lorente-Galdos B, Veeramah KR, Woerner
731 AE, O'Connor TD, Santpere G, et al. 2013. Great ape genetic diversity and population history.
732 *Nature* 499:471–475.
- 733 Robinson JA, Bowie RC, Dudchenko O, Aiden EL, Hendrickson SL, Steiner CC, et al. 2021. Genome-
734 wide diversity in the California condor tracks its prehistoric abundance and decline. *Curr. Biol.*
735 31:2939-2946.e5
- 736 Robinson JT, Turner D, Durand NC, Thorvaldsdóttir H, Mesirov JP, Aiden EL. 2018. Juicebox.js
737 Provides a Cloud-Based Visualization System for Hi-C Data. *Cell Syst* 6:256–258.e1.
- 738 Roesti M. 2018. Varied genomic responses to maladaptive gene flow and their evidence. *Genes* 9:298.
- 739 Sardell JM, Cheng C, Dagilis AJ, Ishikawa A, Kitano J, Peichel CL, Kirkpatrick M. 2018. Sex
740 Differences in Recombination in Sticklebacks. *G3* 8:1971–1983.
- 741 Smalec BM, Heider TN, Flynn BL, O'Neill RJ. 2019. A centromere satellite concomitant with extensive
742 karyotypic diversity across the *Peromyscus* genus defies predictions of molecular drive.
743 *Chromosome Res.* [Internet]. Available from: <http://dx.doi.org/10.1007/s10577-019-09605-1>
- 744 Smith JM, Haigh J. 1974. The hitch-hiking effect of a favourable gene. *Genet. Res.* 23:23–35.
- 745 Smukowski CS, Noor MAF. 2011. Recombination rate variation in closely related species. *Heredity*
746 107:496–508.
- 747 Stankowski S, Chase MA, Fuiten AM, Rodrigues MF, Ralph PL, Streisfeld MA. 2019. Widespread
748 selection and gene flow shape the genomic landscape during a radiation of monkeyflowers. *PLoS*
749 *Biol.* 17:e3000391.
- 750 Stepan SJ, Adkins RM, Anderson J. 2004. Phylogeny and divergence date estimates of rapid radiations
751 in muroid rodents based on multiple nuclear genes. *Syst. Biol.* 53:533-553.
- 752 Tajima F. 1983. Evolutionary relationship of DNA sequences in finite populations. *Genetics* 105:437–
753 460.
- 754 Thybert D, Roller M, Navarro FCP, Fiddes I, Streeter I, Feig C, Martin-Galvez D, Kolmogorov M,
755 Janoušek V, Akanni W, et al. 2018. Repeat associated mechanisms of genome evolution and
756 function revealed by the *Mus caroli* and *Mus pahari* genomes. *Genome Res.* 28:448–459.
- 757 Tigano A, Friesen VL. 2016. Genomics of local adaptation with gene flow. *Mol. Ecol.*, 25: 2144-2164.
- 758 Tigano A, Colella JP, MacManes MD. 2020. Comparative and population genomics approaches reveal
759 the basis of adaptation to deserts in a small rodent. *Mol. Ecol.* 29:1300-1314
- 760 Tigano A, Jacobs A, Wilder AP, Nand A, Zhan Y, Dekker J, Therkildsen NO. 2021. Chromosome-level
761 assembly of the Atlantic silverside genome reveals extreme levels of sequence diversity and
762 structural genetic variation. *Genome Biol. Evol.* 13:evab098
- 763 Van Belleghem SM, Baquero M, Papa R, Salazar C, McMillan WO, Counterman BA, Jiggins CD, Martin
764 SH. 2018. Patterns of Z chromosome divergence among *Heliconius* species highlight the importance

- 765 of historical demography. *Mol. Ecol.* 27:3852–3872.
- 766 Weisenfeld NI, Kumar V, Shah P, Church DM, Jaffe DB. 2017. Direct determination of diploid genome
767 sequences. *Genome Res.* 27:757–767.
- 768 Wiehe TH, Stephan W. 1993. Analysis of a genetic hitchhiking model, and its application to DNA
769 polymorphism data from *Drosophila melanogaster*. *Mol. Biol. Evol.* 10:842–854.
- 770 Yeaman S. 2013. Genomic rearrangements and the evolution of clusters of locally adaptive loci. *Proc.*
771 *Natl. Acad. Sci. U. S. A.* 110:E1743–E1751.
- 772 Yeaman S, Otto SP. 2011. Establishment and maintenance of adaptive genetic divergence under
773 migration, selection, and drift. *Evolution* 65:2123–2129.
- 774

775 **Figures and Tables**

776

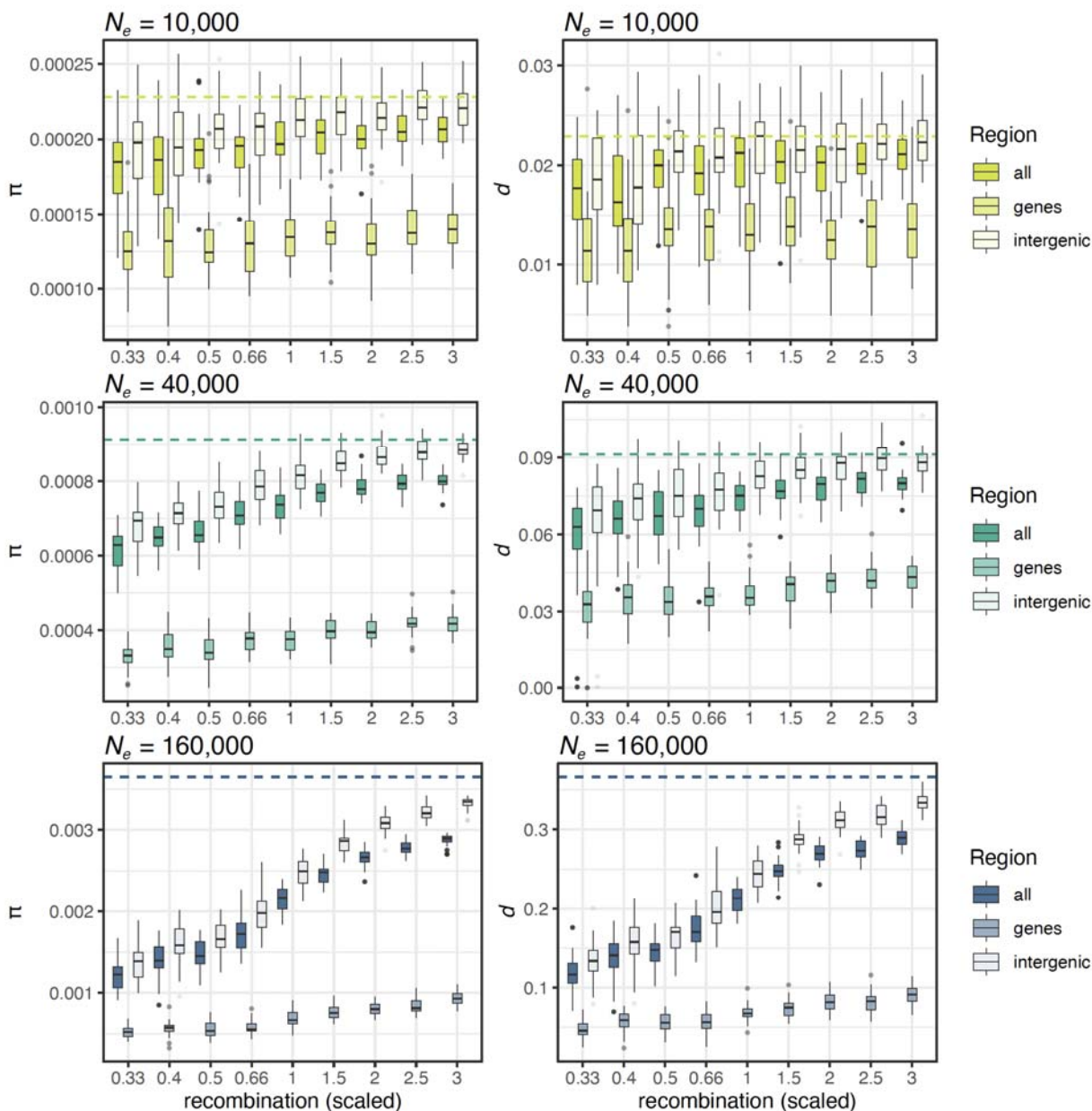
777 **Fig.1.** Plots showing the relationship between \log_{10} -transformed chromosome size (bp) and sequence
778 divergence among species within the *Peromyscus*, Hominidae and *Mus* clades. On the left panel (A, C,
779 E), one representative comparison from each of the *Peromyscus*, Hominidae, and *Mus* clades are
780 displayed (see Figure S2, S3, and S4 for all comparisons). The comparison of the same species pairs are
781 represented on the right panel but the query and reference species are inverted in plots B, D, F to highlight
782 that in the *Mus*, but not in *Peromyscus* and *Hominidae* clades, the choice of the reference genome affects
783 the correlation between chromosome size and d . In the bottom panel, the comparison between *Mus*
784 *spretus* and *M. pahari* is shown, with *M. pahari* as reference on the left (E) and with *M. spretus* as
785 reference on the right (F).



786

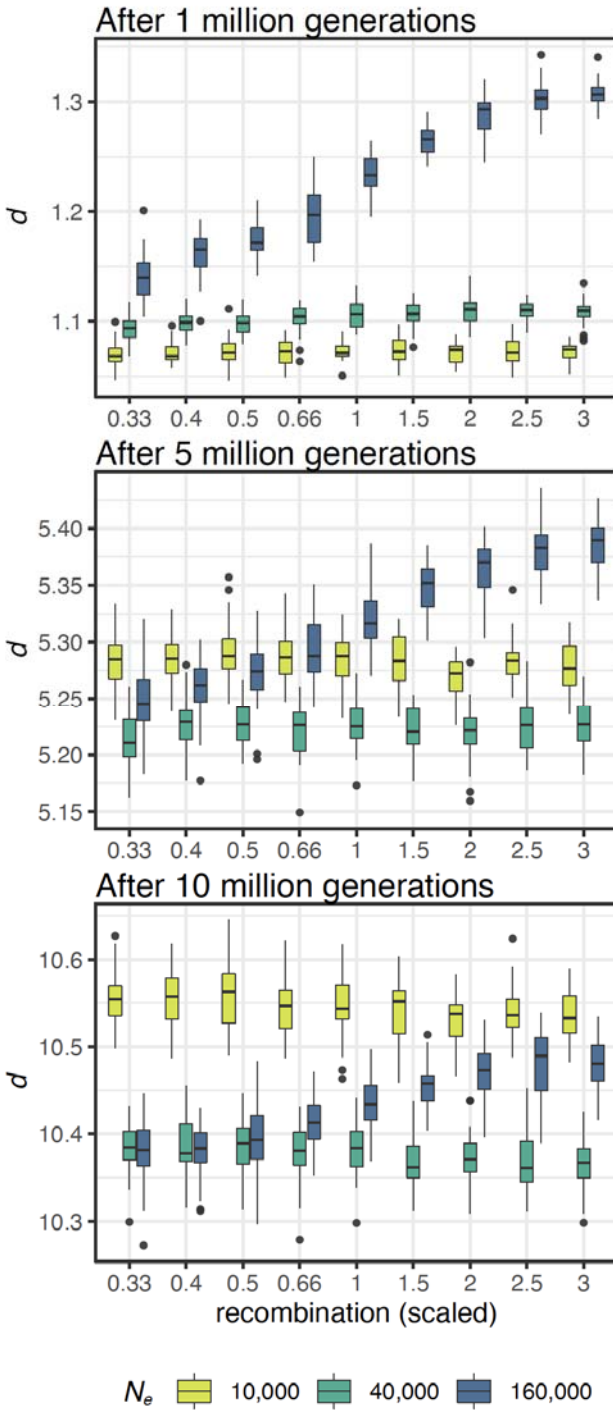
787

788 **Fig. 2.** Boxplots summarizing results from evolutionary simulations on the relationship between
 789 recombination rate and π after $20N_e$ generations in the ancestral population (panel A on the left) and d
 790 one generation after the split after a mild bottleneck (0.5 of ancestral N_e) between the two daughter
 791 populations (panel B on the right) in each of three simulated ancestral N_e . Boxplots refer to the results
 792 from the models with selection and the dashed line shows the results from the neutral models. Here are
 793 the results with models without gene conversion as no significant differences were found between models
 794 with and without gene conversion.



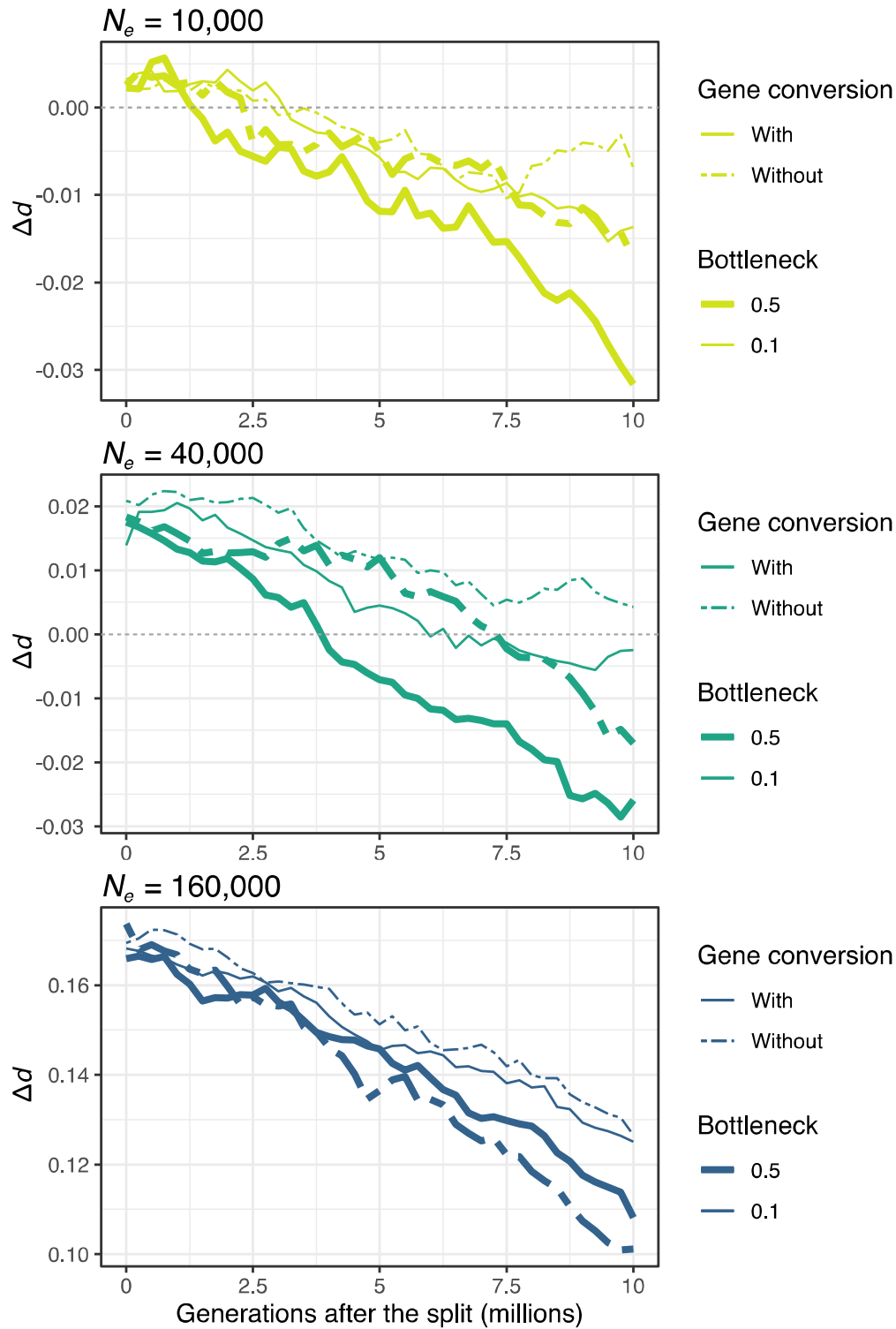
795
 796

797 **Fig. 3.** Boxplots summarizing results from evolutionary simulations on the relationship between
798 recombination rate and d in models with selection and without gene conversion in each of three simulated
799 ancestral N_e and three time points after the split from the ancestral pop_A and a mild bottleneck. Gene
800 conversion was not included in these models as no significant differences were found between models
801 with and without gene conversion. (See Fig. S5 for comparisons with neutral models and models with a
802 more severe bottleneck).



803
804

805 **Fig. 4.** Plots showing the decay of Δd over time in the evolutionary simulations based on the models with
806 and without gene conversion, and with a mild (0.5) and a severe bottleneck (0.1) for each of the three
807 simulated ancestral N_e .



808

809 **Table 1.** Summary of parameters used in evolutionary simulations.

Variable	Values	Scaled values as in simulations (x25)
Mutation rate	$5.7 \cdot 10^{-9}$	$1.42 \cdot 10^{-7}$
Mean recombination rate r	10^{-8}	$2.5 \cdot 10^{-7}$
Gene conversion rate	$r/3$	$r/3$
Gene conversion tract length	440 bp	440 bp
Selection coefficient s	$\pm 15.625 \cdot 10^{-3}$	$\pm 15.625 \cdot 10^{-3}$
Relative frequency of neutral, deleterious, and advantageous mutations	0.3, 1, and 0.0005	0.3, 1, and 0.0005
Selection model	neutral/with selection	neutral/with selection
N_e of pop _A	10,000/40,000/160,000	400/1,600/6,400
Reduction of N_e of pop ₁ and pop ₂ relative to pop _A	0.5/0.1	0.5/0.1
Recombination rates	$0.33r/0.4r/0.5r/0.66r/r/1.5r/2r/2.5r/3r$	$0.33r/0.4r/0.5r/0.66r/r/1.5r/2r/2.5r/3r$
Gene conversion	yes/no	yes/no

810